Identifying Coordination Geometries of Metal Aquaions in Water: Application to the Case of Lanthanoid and Actinoid Hydrates

Noelia Morales, Elsa Galbis, José M. Martínez, Rafael R. Pappalardo, and Enrique Sánchez Marcos*

Department of Physical Chemistry, University of Seville, 41012 Seville, Seville, Spain

E-mail: sanchez@us.es

Phone: +34 955421005

Abstract

The angular distribution function (ADF) associated to the oxygen-metal ion-oxygen angle (OMO) of several trivalent lanthanoid and actinoid aquaions has been used to identify the most probable coordination geometry of these aquaions in aqueous solutions. The ADFs extracted from the Molecular Dynamics trajectories have been compared with continuous distribution functions corresponding to the geometry of a reference polyhedron pattern. The procedure incorporates specific quantum-mechanical information of the aquaion under study. The new method is applied to the analysis of four $M(H_2O)_n^{3+}$ aquaions in water, M=Lu and Cf for n=8, and M=La and Ac for n=9. For those 8-coordinated, the Square Antiprism (SA) coordination geometry is preferred. For the 9-fold coordination the simulation ADFs are more similar to the continuous ADF derived from a Gyro-elongated-SA rather than to the usually proposed Trigonal Tricapped Prism. Advantages of these continuous distributions with respect to the usually employed discrete distributions are emphasized as well as further applications are suggested.

Graphical TOC Entry

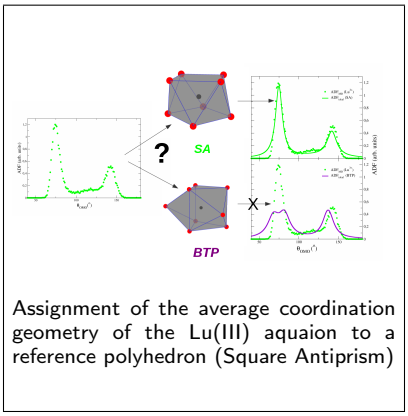

Assignment of the average coordination geometry of the Lu(III) aquaion to a reference polyhedron (Square Antiprism)

Keywords

Broadening model,Octa-coordination, ennea-coordination, polyhedra, Angular distribution functions, Molecular Dynamics, intermolecular potentials

The identification of a metal aquaion structure in solution is not as easy task as one could expect on the basis of the apparently simple distribution of water molecules around a monoatomic cation. Both the natural thermal structural disorder of the liquid state and in addition, sometimes, the water molecules release from the aquaion could make difficult the persistence of a well-defined coordination geometry around a metal ion in solution and, therefore its identification. This is the case of the lanthanoid and actinoid aquaions. Basic knowledge on the actinoid hydration structure and dynamics is important because their role in nuclear technological issues, such as migration in aqueous media of nuclear repositories or the selective extraction agents for the separation of actinoids and lanthanoids.[1]

This contribution presents a new procedure for the identification of the average coordination geometry of a metal aquaion in solution. This methodology is applied to a couple of lanthanoid and actinoid aquaions, which scan the two representative coordination numbers along the series, i.e., the octa- and ennea-coordination.

Relevant experimental techniques, such as neutron and x-ray diffraction methods together with extended x-ray absorption spectroscopy (EXAFS) provide information on metal-water distances, hydration numbers and structural and dynamical disorder.[2–5] Complementary information based on spectroscopies such as IR, Raman, vis-UV or XANES, have widen the available information of aquaions in solution.[4,6] However, the coordination geometry of some aquaions can not be easily assigned. The coordination geometry is often proposed in analogy to crystal structures containing the aquaion or related compounds, as well as from assignment of spectral features which come from a particular type of arrangement based on symmetry reasons.[4,5,7,8] Continuous symmetry measures have been proposed to calibrate the deviation of organometallic compounds from ideal or regular polyhedra.[9,10] Nevertheless, the liquid state presents usually more diffuse coordination geometries around a metal ion in solution, given that there are continuous changes in M-O distances and OMO angles, as a consequence of the intrinsic dynamics of the aquaion. Theoretical methods offer useful tools at the molecular level to tackle this question. The most usual strategy has been the

comparison of the Angle Distribution Function (ADF) of the OMO angles derived from a computer simulation with the discrete distribution exhibited by a reference polyhedron which may be Platonic, Johnson or antiprism.[11–14] There is a significant number of these reference polyhedra for the different coordination numbers ($4 \leq CN \leq 10$) adopted by metal ions in their first hydration shell[3–5] Scheme 1 displays the aquaion structures considering three common reference octa-coordinated polyhedra, Square Antiprism (SA), Cube and Bi-capped Trigonal Prism (BTP), and two ennea-coordination ones, Gyro-elongated Square Antiprism (GySA) and Trigonal Tricapped Prism (TTP). In this study we examine the coordination geometry of some trivalent lanthanoid and actinoid aquaions. It has long been accepted that CN changes from 9 to 8 along the first series,[7,15] whereas for the second series it has been confirmed more recently.[8,16–18] The cations chosen have been La^{3+} and Ac^{3+} as representatives of the 9-coordination, and Lu^{3+} and Cf^{3+} as those of the 8-coordination. The choice of Cf^{3+} is due to the fact that it is the heaviest actinoid for which experimental information in solution has been reported.[17]

The aquaion structures were obtained from classical NVT Molecular Dynamics simulations of systems formed by one trivalent cation and 1000 water molecules. Temperature was set up to 300K and the volume was fixed to reproduce the experimental water density at 1 atm. The flexible and polarizable MCDHO model was employed for the interaction potentials. The water-water potential was proposed by Ortega-Blake and col.[19] and the M^{3+}-H_2O potentials were developed by us as an extension of our hydrated ion model.[20] The model improvements allow the exchange of water molecules between the first hydration shell and the bulk. Details of this new development were previously given for the case of Cf^{3+}.[17,21] For all cations the systematic method B from ref. 21 has been used. The general form of these exchangeable ion-water potentials together with the parameter sets are given in Figure S1 and Table S1 of the Supporting Information (SI). Details on the quantum mechanical (QM) level employed to build the potential energy surfaces are included in Table S2 of SI.

Figure 1 displays the M-O radial distribution functions (RDF). The maximum of the

first peaks shows the splitting of the cations in two groups, those with 8-fold coordination and shorter $R_{\text{M-O}}$ distances, 2.37 Å and 2.44 Å for Lu^{3+} and Cf^{3+}, respectively; and those with 9-fold coordination and longer $R_{\text{M-O}}$ distances, 2.62 Å and 2.65 Å for La^{3+} and Ac^{3+}, respectively. These results agree reasonably well with the experimental and theoretical values available in the literature, which ranges the M-O distance in the interval 2.52-2.65 Å for La^{3+}, 2.30-2.37 Å for Lu^{3+} and 2.37-2.45 Å for Cf^{3+}.[7,8,12,17,18,22–27] A detailed set of structural and energetic properties are collected in Table S3 of the SI, supporting the good behavior of the intermolecular potentials developed.

Plots of the OMO ADFs obtained for the cations from their MD simulations (hereafter $ADF_{MD}(M^{3+})$) are shown in Figure 2. The selected structures to build these ADFs correspond to the snapshots where the hydrate contains either 8 (for Lu^{3+}, it represents 98% of the structures and for Cf^{3+}, 79%) or 9 (for La^{3+}, 89% and for Ac^{3+}, 66%) water molecules. This facilitates the coordination geometry analysis. ADFs were set up by conditioning them to integrate to the total number of OMO angles in the considered CN, i.e. 28 and 36 for the 8-fold and the 9-fold coordinations, respectively. It is observed that $ADF_{MD}(M^{3+})$s of a given CN are very similar regardless the cation considered. This is also confirmed by the analysis of the 34% of the structures which correspond to Ac^{3+} octa-coordinated which yields the same ADF_{MD} than the other octacoordinated cations. However, the profiles for both CNs have two main differences: peak separation and peak intensity ratio for the 8-coordination are larger than for the 9-coordination ones.(See Figure 2)

The usual procedure to associate a coordination geometry to a particular ADF_{MD} has been its comparison with the discrete angle distribution provided by a reference polyhedron of the same CN. Figure 3(top) displays the $ADF_{MD}(La^{3+})$ and the discrete distributions derived for the two reference 9-fold coordinated polyhedra shown in Scheme 1: the GySA and the TTP ones. Figure 3(bottom) displays the $ADF_{MD}(Cf^{3+})$ and the discrete distributions corresponding to the SA, Cube and BTP polyhedra. This figure shows the difficulty to associate a given polyhedron to an $ADF_{MD}(M^{3+})$. Thus, for the La^{3+} case, both GySA and

TTP discrete distributions accumulate their higher intense lines around the two main peaks of the $ADF_{MD}(La^{3+})$, but there is not a clear indication to choose between the two discrete distributions. In the Cf^{3+} case (Figure 3 (bottom)), it seems clear that the Cube discrete distribution is far from the $ADF_{MD}(Cf^{3+})$, but it is also unclear the assignment to the BTP or SA polyhedron, where a significant contribution appears at 119° whereas the ADF_{MD} exhibits a depletion in the 90°-130° range.

To facilitate the assignment we have established a procedure to build a specific continuous angle distribution of a reference polyhedron based on quantum mechanical information derived from the corresponding aquaion. Broadening methods in spectroscopy have long been used to account for the different sources of spectroscopic line broadening. In this study we have chosen Lorentzian functions (Eq.1) to be centered on each of the OMO angle values (θ_0) of the reference polyhedron.

$$\mathcal{L}_{\theta_o}(\theta) = \frac{A}{\pi} \frac{\Gamma}{2(\theta - \theta_o)^2 + \frac{\Gamma^2}{4}} \tag{1}$$

Γ parameter defines the Lorentzian width which will be associated to $\Delta\theta_{\mathrm{FWHH}}$, i.e. the full width at half height of a given peak centered at θ_o. The third Lorentzian parameter to be assigned is A, a multiplier which guarantees that the integration of the Lorentzian renders the number of OMO angles associated to a given θ_o value.

We propose to relate the Γ parameter of a given angle distribution centered at θ_o to the force constant of the bending normal mode associated to the set of atoms involved in the definition of angle θ. To quantify this force constant, a quantum mechanical calculation of the considered aquaion structure is performed at the computational level employed for the development of the intermolecular potential. Due to the large number of bending normal modes involving the different angles, an average force constant ($\overline{k}$) associated to the set of structurally-related bending normal modes has been used. Table S4 in SI collects the $\overline{k}$ values used for the polyhedra which are minima on the corresponding potential energy surface of the aquaions, i.e. SA and TTP. In order to include the solvent effects, the Γ value is related

to the width of the corresponding ADF_{MD} peak (Figure 2).

Let us consider the SA case (see Scheme 1) where there are 28 OMO angles distributed among three different angle values: 75°, 119° and 142° with appearance frequencies of 16:4:8, respectively. To establish the relationship between the $\Delta\theta_{FWHH}$ and $\overline{k}$, the simplest case of the $ADF_{MD}(Cf^{3+})$ and the SA discrete distribution (Figure 3 (bottom)) is analyzed. The two $ADF_{MD}(Cf^{3+})$ peaks centered at 74.0° and 143.0° can be associated to the discrete lines of the reference SA polyhedron at 75° and 142°, with $\Delta\theta_{FWHH}$ values of 12.5° and 16.2°, respectively. Quite similar values are associated to the Lu^{3+} case, as shown in Table S4 in SI. The examination of the set of $\overline{k}$ and $\Delta\theta_{FWHH}$ values for these two aquaions suggests an useful relationship between them:

$$\bar{k} \times \Delta\theta_{FWHH} = constant \tag{2}$$

where the *constant* value, 0.6134 hartree degrees $Å^{-2}$, is derived from the average of the Cf^{3+} and Lu^{3+} data. Eq. (2) is useful for the adscription of the $\Delta\theta_{FWHH}$ value to a reference polyhedron angle which does not have a peak associated in the $ADF_{MD}(Cf^{3+})$, as it is the case of the intermediate angle 119°. Then, Eq. (2) and the corresponding QM force constant, k_{119}, given in Table S4, provide a way to set $\Delta\theta_{FWHH}(119°)$ values of 87.6° and 73.0° for Cf^{3+} and Lu^{3+}, respectively. Regarding the A values for the SA case, the Lorentzian function associated to θ_0= 75° must integrate to 16, then A_{75} must take such a value that this condition is satisfied. The continuous ADF for a reference polyhedron, $\mathcal{L}_{total}$, (hereafter termed ADF_{cont}) is defined as the sum of the different Lorentzians, $\mathcal{L}_{\theta_o}$, centered at the different θ_o angles.

$$\mathcal{L}_{total} = N(\mathcal{L}_{75} + \mathcal{L}_{119} + \mathcal{L}_{142}) \tag{3}$$

$\mathcal{L}_{total}$ must be renormalized by means of N to give an integration value in the existence angle range of the $ADF_{MD}(M^{3+})$ equals to 28 or 36, i.e. the total number of angles

appearing in the octa-coordinated or ennea-coordinated reference polyhedron, respectively (see Figure S2).

Figure 4 shows the comparison of the $ADF_{MD}(Cf^{3+})$ and $ADF_{MD}(Lu^{3+})$ with the ADF_{cont} generated from the three reference polyhedra associated to the octa-coordination. In the case of the Cube and BTP polyhedra their geometries are not minima in the potential energy surface of the corresponding aquaions. It is worth commenting on this point that the preferred coordination geometry for the isolated aquaion is not necessarily the most favoured in solution due to the solvent effects. Their Γ values have been taken from the SA Cf^{3+} Lorentzians, associating the same SA Γ value to the Cube or BTP Lorentzian of an structurally-related angle. Values have been collected in Table S4 of SI. $ADF_{MD}(Cf^{3+})$ and $ADF_{MD}(Lu^{3+})$ are very similar to ADF_{cont}(SA). This confirms the usually assigned arrangement for $[M(H_2O)_8]^{3+}$, both in crystals and in aqueous solution.[11] Interestingly the ADF_{cont}(Cube) and the ADF_{cont}(SA) are quite different, even though both arrangements only differ in the relative 45° rotation of one of the oxygen-atom square plane with respect to the other (see Scheme 1). For the same M-O distances, their M-O RDFs would match. This is an illustrative example of the sensitivity of this methodology to coordination symmetry changes. The ADF_{cont}(BTP) may also be discarded as coordination geometry.

For the ennea-coordinated aquaions, La^{3+} and Ac^{3+}, Figure 3 shows that different discrete distributions from the TTP and GySA reference polyhedra contribute to each peak of the ADF_{MD}, unlike the 8-fold coordination SA case. Then, it is assumed that the relationship of eq. (2) can be applied to assign the Lorentzian width. Table S4 in SI collects the parameters employed for the different Lorentzians based on the QM calculations for the TTP minimum of La^{3+}. The GySA is not a minimum and its Lorentzians have been obtained from the structurally related TTP angles. Given the high similarity between the La^{3+} and Ac^{3+} ADF_{MD}s, a common ADF_{cont} have been built for both cations. Figure 5 displays the ADF_{MD}s for La^{3+} and Ac^{3+}, together with the ADF_{cont}(TTP) and ADF_{cont}(GySA) polyhedra. The comparison for the ennea-coordination shows the similarity of ADF_{MD}s for

both the La^{3+} and Ac^{3+} aquaions to the ADF_{cont}(GySA). This result is against the usual previous TTP assignment in solution, supported by evidences of some crystals structures containing the ennea-hydrated cation.[5,13,14,28,29] Nevertheless, some authors, based on discrete angular distribution analysis, had already pointed out difficulties to discard the GySA arrangement, due to the thermal fluctuations in the liquid medium.[11,13,14] Kowall et al.[11] compute a continuous ADF by broadening the angle discrete lines using a Gaussian function without including quantum-mechanical information. In this study we have shown that the specificity provided by the QM computations is critical to smear out spurious contributions at θ values between the two main peaks centered at $\sim 75^\circ$ and $\sim 140^\circ$. Additionally, the overall peak shape is also modelled by the Lorentzian sum, $\mathcal{L}_{\text{total}}$.

Once the ADF broadening model has been detailed, one could wonder if the selection of Lorentzian functions may condition the results. To answer this question we have used Gaussian functions to compute ADF_{cont}, applying the same procedure to select the function parameters. Results are given in Figure S3 of SI. The examination of ADF_{cont} for SA and TTP obtained from Gaussians leads to the same conclusions reached from Lorentzians.

The mean residence times of the first-shell water molecules of these aquaions are 320 ps for La^{3+} and 870 ps for Lu^{3+}.[30] This means that in the particular case of the lanthanoids and actinoids studied, the main factor affecting the consistency of the aquaions is the intrinsic dynamics of the ion and its first hydration shell. One could revise the structural requirement for TTP in solution based on the persistence of a double set of M–O distances (6+3) corresponding to its equatorial and axial arrangement. The expected distance distribution is not observed in the M-O RDFs (Figure 1). Distance fluctuations are high enough to smear out differential peaks in the global RDF. Likewise, histograms of M-O distances for the 8-(Lu^{3+}) and 9-coordinated (La^{3+}) shows the impossibility to assign the reference polyhedra solely using the pattern of distance sets found in them (Figure S4). Continuous ADF appear to be more sensitive to discriminate the coordination geometry.

The preference for a GySA arrangement provided by the ADF analysis opens the way

to a plausible 9-fold coordination model: let us consider a robust and symmetrized SA arrangement with the coupling of a ninth water molecule facing one of the square planes, playing the role of an *apical* water molecule (see GySA in Scheme 1). This picture is appropriate to supply a new view of the series of lanthanoid and actinoid aquaions, and the CN along the series. The basic idea is that the symmetric SA arrangement is the most structurally-consistent aquaion and the axial approach of a ninth water molecule to the external side of one of the square-planar faces, smoothly provides a partial contribution to the total coordination from 0 to 1. The partial contribution may be a function of the physicochemical properties of the lanthanoid or actinoid cation considered.

Thus, the specific properties of a given cation plus its basic SA structure along the series confer different inter-molecular interactions with the ninth water molecule, which will give in an average manner, a contribution between one and nill to the octa-coordination provided by the SA arrangement. It is worth commenting on the similar pattern already found in the closest hydration structure of square-planar Pd(II) and Pt(II) complexes, where a *meso-shell* in the axial regions was identified.[31–34]

Electrolyte aqueous solutions are not noisy crystalline solids. Their intrinsic thermal structural disorder offers their own landscape which must be contemplated from a different viewpoint. This work must be considered as an starting point of further studies which must get a deeper insight into the dynamical properties of the apical water molecules in solution.

Further studies of other frequent coordination numbers may be examined with this methodology, extending the potential ability of the proposed method to other coordination geometry problems of solution chemistry, involving metal aquaions, such as the chemically relevant coordinations 10, 7 or 6. They are matter of ongoing debate, such as the Cu^{2+} aquaion case,[35–38] or the recently revisited case of the Sc^{3+} aquaion.[39] Moreover, the extension of this ADF broadening method to coordination compounds could be regarded as an useful further step in the geometrical characterization of them in solution.

Acknowledgement

Authors acknowledge the Junta de Andalucia for financial support (P11-FQM7607). NM thanks for a Ph.D. grant to Spanish Ministry of Economy and Competitiveness (Project number CTQ2011-25932).

Supporting Information Available

Methodology on the building of the intermolecular ion-water potentials and the fitted parameters potentials for the four cations, quantum mechanical information on the computed potential energy surfaces, molecular dynamics simulation conditions, structural data derived from MD simulations, M-O distance Histograms, example of the procedure to obtain a continuous ADF for a reference polyhedron, continuous ADF obtained from the use of Gaussians, data of Lorentzians employed in the construction of continuous ADFs. This material is available free of charge via the Internet at `http://pubs.acs.org/`.

References

(1) Nash, K.; Madic, C.; Mathur, J. N. In *The Chemistry of the Actinide and Transactinide Elements*; Morss, L. R., Edelstein, N. M., Fuger, J., Katz, J. J., Eds.; Springer: Dordrecht, 2006; Vol. 4; Chapter 24.

(2) Magini, M.; Piccaluga, G.; Paschina, G.; Pinna, G. *X-Ray Diffraction of Ions in Aqueous Solutions: Hydration and Complex Formation*; CRC Press: Boca Raton, 1988.

(3) Ohtaki, H.; Radnai, T. Structure and Dynamics of Hydrated Ions. *Chem. Rev.* **1993**, *93*, 1157–1204.

(4) Richens, D. T. *The Chemistry of Aqua Ions*; John Wiley: Chichester, 1997.

(5) Persson, I. Hydrated Metal Ions in Aqueous Solution: How Regular Are Their Structures? *Pure. Appl. Chem.* **2010**, *82*, 1901–1917.

(6) Penner-Hahn, J. E. X-Ray Absorption Spectroscopy in Coordination Chemistry. *Coord. Chem. Rev.* **1999**, *190-192*, 1101–1123.

(7) Persson, I.; D'Angelo, P.; Panfilis, S. D.; Sandström, M.; Eriksson, L. Hydration of Lanthanoid(III) Ions in Aqueous Solution and Crystalline Hydrates Studied by EXAFS Spectroscopy and Crystallography: The Myth of the "Gadolinium Break". *Chem. Eur. J.* **2008**, *14*, 3056–3066.

(8) Apostolidis, C.; Schimmelpfenning, B.; Magnani, N.; Lindqvist-Reis, P.; Walter, O.; Sykora, R.; Morgenstern, A.; Colineau, E.; Caciuffo, R.; Klenze, R. et al. $[An(H_2O)_9](CF_3SO_3)_3$ (An=U,Cm, Cf): Exploring Their Stability, Structural Chemistry, and Magnetic Behavior by Experiment and Theory. *Angew. Chem. Int. Ed.* **2010**, *49*, 6343–6347.

(9) Alvarez, S.; Alemany, P.; Casanova, D.; Cirera, J.; Llunell, M.; Avnir, D. Shape Maps and Polyhedral Interconversion Paths in Transition Metal Chemistry. *Coord. Chem. Rev.* **2005**, *249*, 1693–1708.

(10) Alvarez, S.; Menjón, B.; Casanova, D.; Falceto, A.; Alemany, P. Stereochemistry of Complexes with Double and Triple Metal-Ligand Bonds: A Continuous Shape Measures Analysis. *Inorg. Chem.* **2014**, *53*, 12151–12163.

(11) Kowall, T.; Foglia, F.; Helm, L.; Merbach, A. E. Molecular Dynamics Simulation Study of Lanthanide Ions Ln^{3+} in Aqueous Solution. Analysis of the Structure of the First Hydration Shell and of the Origin of Symmetry Fluctuations. *J. Phys. Chem.* **1995**, *99*, 13078–13087.

(12) Hofer, T.; Scharnagl, H.; Randolf, B.; Rode, B. Structure and Dynamics of La(III)

in Aqueous Solution - an Ab Initio QM/MM MD Approach. *Chem. Phys.* **2006**, *327*, 31–42.

(13) Duvail, M.; Souaille, M.; Spezia, R.; Cartailler, T.; Vitorge, P. Building a Polarizable Pair Interaction Potential for Lanthanoids(III) in Liquid Water: A Molecular Dynamics Study of Structure and Dynamics of the Whole Series. *J. Chem. Phys.* **2007**, *127*, 034503.

(14) Atta-Fynn, R.; Bylaska, E. J.; Schenter, G.; de Jong, W. Hydration Shell Structure and Dynamics of Curium(III) in Aqueous Solution: First Principles and Empirical Studies. *J. Phys. Chem. A* **2011**, *115*, 4665–4677.

(15) D'Angelo, P.; Panfilis, S. D.; Filipponi, A.; Persson, I. High-Energy X-Ray Absorption Spectroscopy: A New Tool for Structural Investigations of Lanthanoids and Third-Row Transition Elements. *Chem. Eur. J.* **2008**, *14*, 3045–3055.

(16) Hagberg, D.; Bednarz, E.; Edelstein, N. M.; Gagliardi, L. A Quantum Chemical and Molecular Dynamics Study of the Coordination of Cm(III) in Water. *J. Am. Chem. Soc.* **2007**, *129*, 14136–14137.

(17) Galbis, E.; Hernández-Cobos, J.; den Auwer, C.; Naour, C. L.; Guillaumont, D.; Simoni, E.; Pappalardo, R. R.; Sánchez Marcos, E. Solving the Hydration Structure of the Heaviest Actinide Aqua Ion Known: The Californium(III) Case. *Angew. Chem. Int. Ed.* **2010**, *22*, 3811–3815.

(18) D'Angelo, P.; Martelli, F.; Spezia, R.; Filipponi, A.; Denecke, M. A. Hydration Properties and Ionic Radii of Actinide(III) Ions in Aqueous Solution. *Inorg. Chem.* **2013**, *52*, 10318–10324.

(19) Saint-Martin, H.; Hernández-Cobos, J.; Bernal-Uruchurtu, M. I.; Ortega-Blake, I.; Berendsen, H. J. C. A Mobile Charge Densities in Harmonic Oscillators (MCDHO)

Molecular Model for Numerical Simulations: The Water-Water Interaction. *J. Chem. Phys.* **2000**, *113*, 10899–10912.

(20) (a) Pappalardo, R. R.; Sánchez Marcos, E. Recovering the Concept of the Hydrated Ion for Modeling Ionic Solutions: A Monte Carlo Study of Zn^{2+} in Water. *J. Phys. Chem.* **1993**, *97*, 4500–4504; (b) Martínez, J. M.; Pappalardo, R. R.; Sánchez Marcos, E. A Molecular Dynamics Study of the Cr^{3+} Hydration Based on a Fully Flexible Hydrated Ion Model. *J. Chem. Phys.* **1998**, *109*, 1445–1455; (c) Martínez, J. M.; Pappalardo, R. R.; Sánchez Marcos, E. First-Principles Ion-Water Interaction Potentials for Highly Charged Monatomic Cations. Computer Simulations of Al^{3+}, Mg^{2+}, and Be^{2+} in Water. *J. Am. Chem. Soc.* **1999**, *121*, 3175–3184.

(21) Galbis, E.; Hernández-Cobos, J.; Pappalardo, R. R.; Sánchez Marcos, E. Collecting High-Order Interactions in an Effective Pairwise Intermolecular Potential Using the Hydrated Ion Concept: The Hydration of Cf^{3+}. *J. Chem. Phys.* **2014**, *140*, 214104.

(22) Habenschuss, A.; Spedding, F. H. The Coordination (hydration) of Rare Earth Ions in Aqueous Chloride Solutions from X-Ray Diffraction. III. $SmCl_3$, $EuCl_3$, and Series Behavior. *J. Chem. Phys.* **1980**, *73*, 442–450.

(23) Duvail, M.; Vitorge, P.; Spezia, R. Building a Polarizable Pair Interaction Potential for Lanthanoids(III) in Liquid Water: A Molecular Dynamics Study of Structure and Dynamics of the Whole Series. *J. Chem. Phys* **2009**, *130*, 104501(1)–104501(13).

(24) Yamaguchi, T.; Nomura, M.; Wakita, H.; Ohtaki, H. An Extended X-ray Absorption Fine Structure Study of Aqueous Rare Earth Perchlorate Solutions in Liquid and Glassy States. *J. Chem. Phys.* **1988**, *89*, 5153–5159.

(25) Revel, R.; den Auwer, C.; Madic, C.; David, F.; Fourest, B.; Hubert, S.; Le Du, J.-F.; Mors, L. R. First Investigation on the L Edges of the ^{249}Cf Aquo Ion by X-Ray Absorption Spectroscopy. *Inorg. Chem.* **1999**, *38*, 4139–4141.

(26) Villa, A.; Hess, B.; Saint-Martin, H. Dynamics and Structure of Ln(III)-Aqua Ions: A Comparative Molecular Dynamics Study Using Ab Initio Based Flexible and Polarizable Model Potentials. *J. Phys. Chem. B* **2009**, *113*, 7270 – 7281.

(27) D'Angelo, P.; Zitolo, A.; Migliorati, V.; Chillemi, G.; Duvail, M.; Vitorge, P.; Abadie, S.; Spezia, R. Revised Ionic Radii of Lanthanoid(III) Ions in Aqueous Solution. *Inorg. Chem.* **2011**, *50*, 4572–4579.

(28) Chaussedent, S.; Monteil, A.; Ferrari, M.; Longo, L. D. Molecular Dynamics Study of Eu^{3+} in an Aqueous Solution: Luminescence Spectrum from Simulated Environments. *Philos. Mag. B* **1998**, *77*, 681–688.

(29) Lindqvist-Reis, P.; Apostolidis, C.; Rebizant, J.; Morgenstern, A.; Klenze, R.; Walter, O.; Fanghänel, T.; Haire, R. The Structures and Optical Spectra of Hydrated Transplutonium Ions in the Solid State and in Solution. *Angew. Chem. Int. Ed.* **2007**, *46*, 919–922.

(30) Helm, L.; Merbach, A. Inorganic and Bioinorganic Solvent Exchange Mechanisms. *Chem. Rev.* **2005**, *105*, 1923–1960.

(31) Martínez, J. M.; Torrico, F.; Pappalardo, R. R.; Sánchez Marcos, E. Understanding the Hydration Structure of Square-Planar Aquaions: the $[Pd(H_2O)_4]^{2+}$ Case. *J. Phys. Chem. B* **2004**, *108*, 15851–15855.

(32) Purans, J.; Fourest, B.; Cannes, C.; Sladkov, V.; David, F.; Venault, L.; Lecomte, M. Structural Investigation of Pd(II) in Concentrated Nitric and Perchloric Acid Solutions by XAFS. *J. Phys. Chem. B* **2005**, *109*, 11074–11082.

(33) Truflandier, L. A.; Autschbach, J. Probing the Solvent Shell with ^{195}Pt Chemical Shifts: Density Functional Theory Molecular Dynamics Study of Pt(II) and Pt(IV) Anionic Complexes in Aqueous Solution. *J. Am. Chem. Soc.* **2010**, *132*, 3472–3483.

(34) Bowron, D. T.; Beret, E. C.; Martin-Zamora, E.; Soper, A. K.; Sánchez Marcos, E. Axial Structure of the Pd(II) Aqua Ion in Solution. *J. Am. Chem. Soc.* **2012**, *134*, 962–967.

(35) Pasquarello, A.; Petri, I.; Salmon, P. S.; Parisel, O.; Car, R.; Tï£¡th, E.; Powell, D. H.; Fischer, H. E.; Helm, L.; Merbach, A. E. First Solvation Shell of the Cu(II) Aqua Ion: Evidence for Fivefold Coordination. *Science* **2001**, *291*, 856–859.

(36) Frank, P.; Benfatto, M.; Szilagyi, R. K.; D'Angelo, P.; Longa, S. D.; Hodgson, K. O. The Solution Structure of $[Cu(aq)]^{2+}$ and Its Implications for Rack-Induced Bonding in Blue Copper Protein Active Sites. *Inorg. Chem.* **2005**, *44*, 1922–1933.

(37) Chaboy, J.; Muñoz-Paez, A.; Merkling, P. J.; Sánchez Marcos, E. The Hydration of Cu^{2+}: Can the Jahn-Teller Effect Be Detected in Liquid Solution? *J. Chem. Phys.* **2006**, *124*, 064509.

(38) Penna, G. L.; Minicozzi, V.; Morante, S.; Rossi, G. C.; Stellato, F. A First-Principle Calculation of the XANES Spectrum of Cu^{2+} in Water. *J. Chem. Phys.* **2015**, *143*, 124508.

(39) Migliorati, V.; D'Angelo, P. Unraveling the Sc^{3+} Hydration Geometry: The Strange Case of the Far-Coordinated Water Molecule. *Inorg. Chem.* **2016**, *55*, 6703–6711.

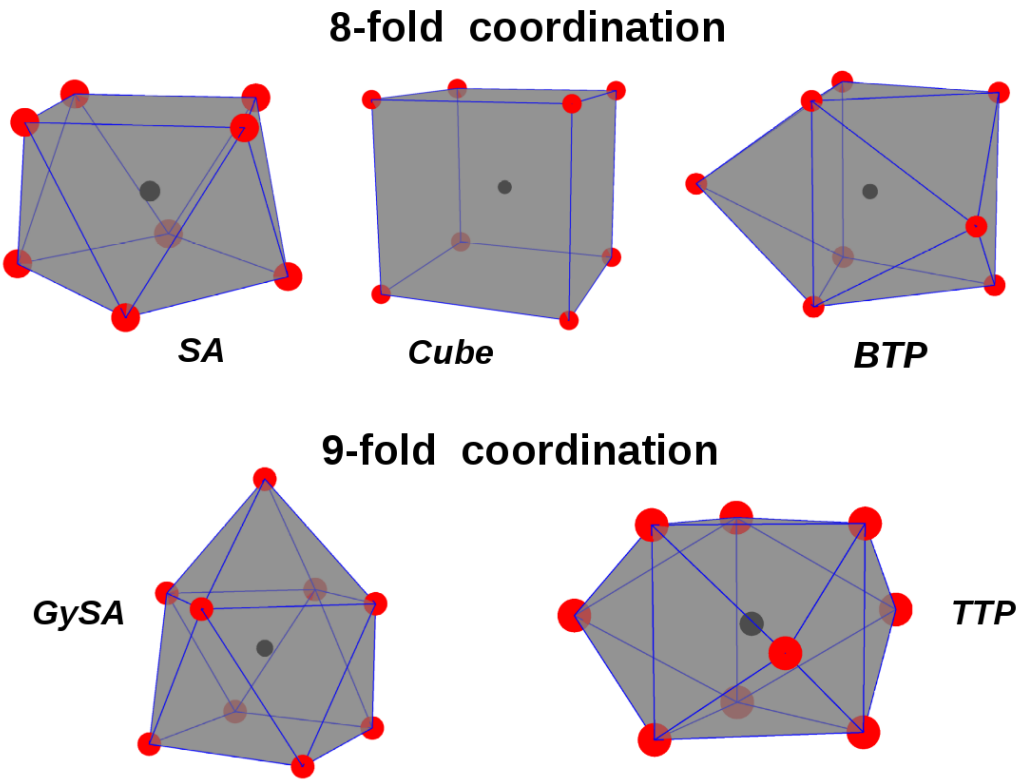

Scheme 1: Models of 8-fold and 9-fold coordination for aquaions where the oxygen atoms are placed on the vertices of a reference polyhedron: SA, Cube and BTP for the octa-coordination and GySA and TTP for the ennea-coordination.

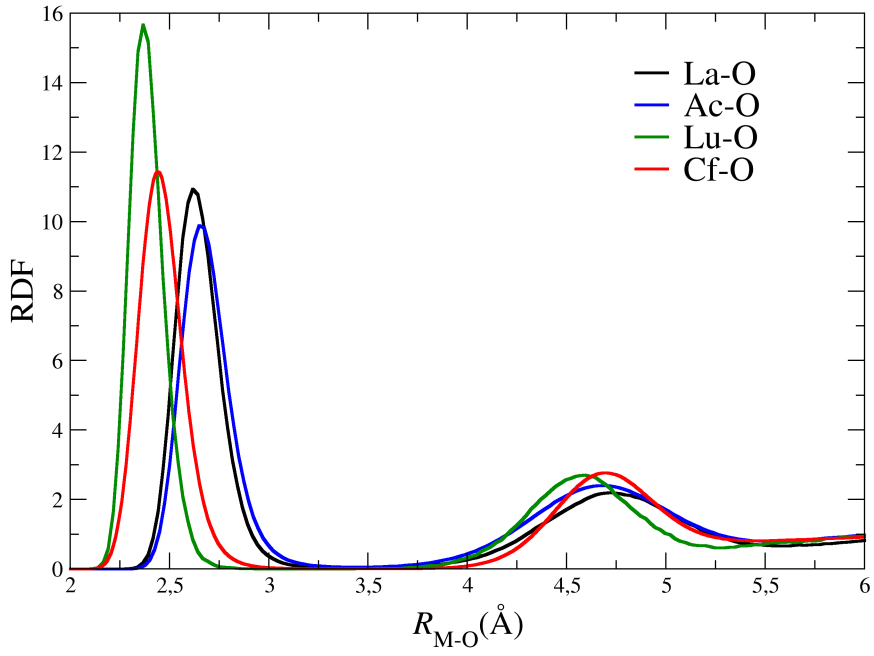

Figure 1: M–O RDFs obtained from the MD simulations of the trivalent cations in aqueous solution

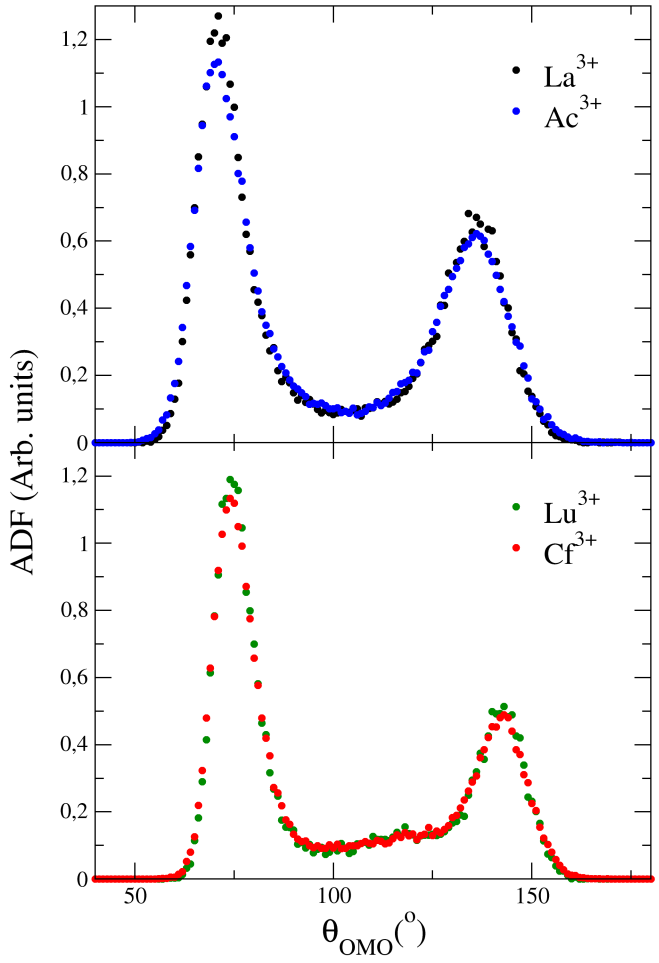

Figure 2: ADFs obtained from the MD simulations of the trivalent cations in aqueous solution

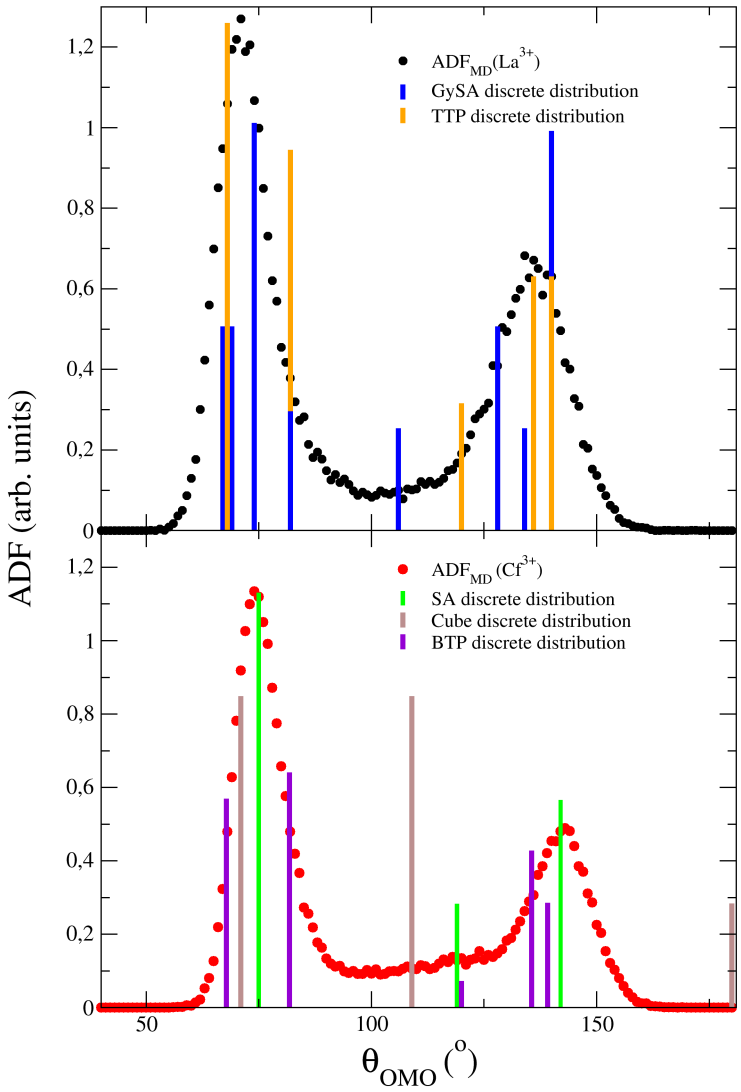

Figure 3: ADF obtained from the MD simulations of the La^{3+} (top) and Cf^{3+} (bottom) in aqueous solution compared to the discrete distributions of reference polyhedra.

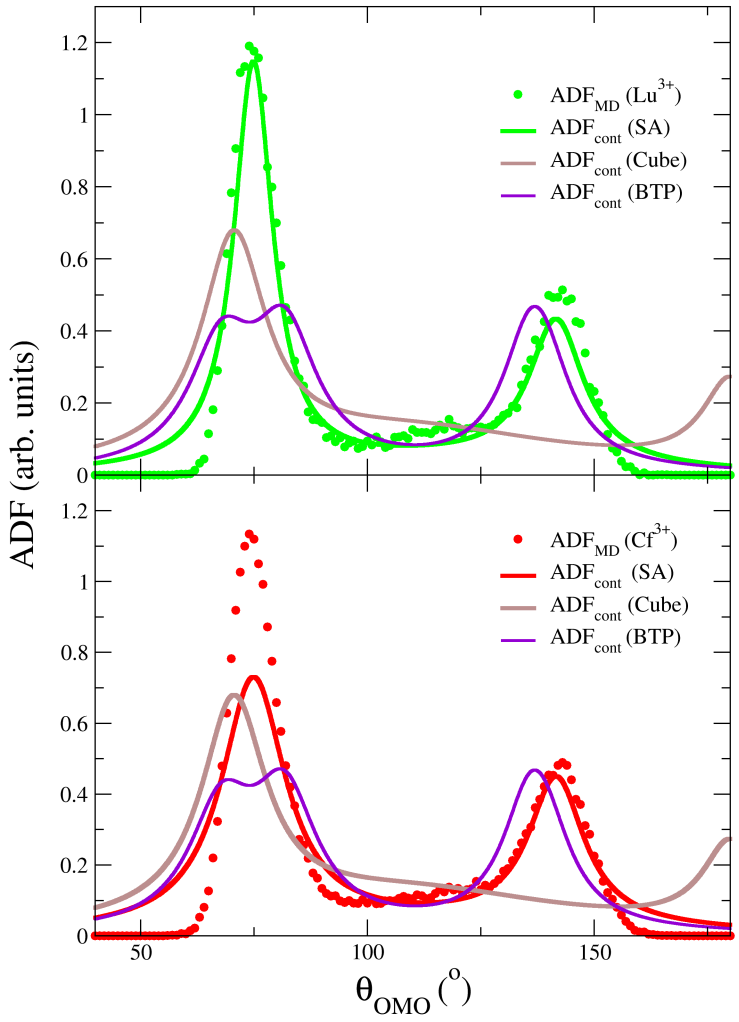

Figure 4: Comparison of the simulation ADFs for Lu^{3+} (top) and Cf^{3+} (bottom) and the ADF_{cont} for the SA, Cube, and BTP 8-coordination polyhedra

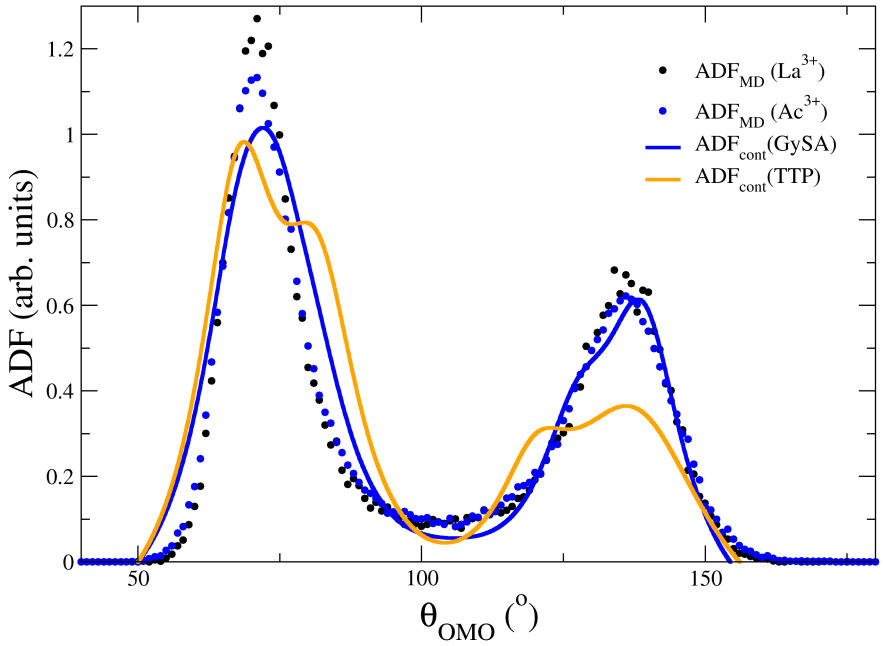

Figure 5: Comparison of the simulation ADFs for La^{3+} (black dot) and Ac^{3+} (blue dot) and the ADF$_{cont}$s for the GySA (blue line) and TTP (orange line) 9-coordination polyhedra